

# Production of CH<sub>4</sub> and C<sub>2</sub> hydrocarbons by axial and radial pulse H<sub>2</sub>/CO<sub>2</sub> discharges with Ni catalysis

Fumiaki Sato, Satoru Iizuka

Graduate School of Engineering, Tohoku University, Sendai, Miyagi 980-8579, Japan

## ABSTRACT

Production of methane CH<sub>4</sub> from a mixture gas of carbon dioxide CO<sub>2</sub> and hydrogen H<sub>2</sub> has been established by two types of pulse discharges. One is an axial discharge with a use of thin pair Ni wire electrodes separated by a narrow gap, and the other is a coaxially radial discharge with a use of inner rod and outer tube electrodes made of stainless steel (SUS). The former provides an intense gap discharge, while the latter provides a gentle discharge in the annular region. Decomposition of CO<sub>2</sub> is enhanced in the former case when Ni (nickel) mesh disc electrode is placed behind the gap. Ni is known as catalysis. When the radial discharge proceeds in a closed gas system, 2C hydrocarbons such as ethane and ethylene are generated in case that a cylindrical mesh electrode made of Ni is attached to the powered SUS tube electrode. Both of the CH<sub>4</sub> production and the energy efficiency for CH<sub>4</sub> production are enhanced in case of Ni mesh electrodes, without a use of additional heating for the Ni catalysis. Synergy effect of plasma and Ni catalyst is observed.

**Keywords** - Carbon dioxide, methane, hydrogen plasma, pulse discharge, Ni catalysis, 2C hydrocarbons.

Date of Submission: 19 January 2017



Date of Accepted: 20 February 2017

## I. INTRODUCTION

It is clear that fossil fuel reserves are finite. If we continue to consume oil, for example, crude oil reserves are vanishing at the rate of 4 billion tons a year, which may result in oil deposits gone by 2052 [1]. An increase in natural gas production to fill the energy gap left by oil will also result in its vanishing by 2060. The coal deposits we know about will only give us enough energy as far as 2088 [1]. Further, another problem comes up, i.e., CO<sub>2</sub> emission from burning fossil fuels. It is well known that CO<sub>2</sub> is a greenhouse gas. The amount of radiation which escapes from the earth depends on the concentration of greenhouses gases in the atmosphere. The increase in CO<sub>2</sub> in the atmosphere will cause an increase in the surface temperature of the earth, which could have disastrous consequences, such as sea level rise, reduction of the ozone layer, increased extreme weather, spread of diseases, and ecosystem change. In this way, the effect of CO<sub>2</sub> emissions by the consumption of fossil fuels could be extremely far reaching and cause major energy and environmental problems [2]. To solve these problems, reusable energy such as solar power is desirable. To suppress CO<sub>2</sub> emission into the environment from electrical power plants, for example, it could be possible that CO<sub>2</sub> is collected and converted to CH<sub>4</sub> before exhausting, if any surplus renewable electric power exists. Methane is a main component of natural gas and can be used as raw materials in the chemical engineering. This means that the surplus renewable energy can be stored as CH<sub>4</sub> [3, 4].

Production of CH<sub>4</sub> from CO<sub>2</sub> is rather easily established by hydrogen discharge plasmas [5-12]. However, a little work has been reported for CH<sub>4</sub> production from a mixture gas of CO<sub>2</sub>/H<sub>2</sub>. In most cases, CO<sub>2</sub> was reduced by CH<sub>4</sub> to produce syngas of CO and H<sub>2</sub>, because methane is also one of the greenhouse gases [13-20]. The production of CH<sub>4</sub> was studied by a dielectric barrier discharge with H<sub>2</sub> in detail [5], where mixed gas of CO<sub>2</sub> and H<sub>2</sub> was employed for CH<sub>4</sub> production. However, for an efficient formation of methane a new innovative method has been expected.

The generation of CH<sub>4</sub> from a mixture gas of CO<sub>2</sub> and H<sub>2</sub> is known as Sabatier reaction in the chemical engineering [21]. By employing catalysis such as Ni (nickel), CH<sub>4</sub> was generated under high pressure and high temperature (200- 400 K) condition, where decomposition of CO<sub>2</sub> was carried out on the catalysis surface [21-23]. On the other hand, in a combined system of plasma and catalysis, which we intend to develop, CO<sub>2</sub> can be easily decomposed by plasma electrons, together with decomposition of H<sub>2</sub>. The produced reactive species such as CO<sup>\*</sup> and H<sup>\*</sup> in the discharge might be available for relaxing the severer reaction condition on the catalysis surface if such plasma and catalysis reaction system is employed.

The purpose of this study is to investigate fundamental process of the reduction of CO<sub>2</sub> by hydrogen radicals that were produced in CO<sub>2</sub>/H<sub>2</sub> discharge [24-28]. Here, we compare two type discharges, i.e., a discharge in the axial direction (axial discharge) and a discharge in the radial direction (radial discharge), with a use of Ni

catalysis for efficient methane production. Our method proposed here is quite unique for a production of reusable organic materials,  $\text{CH}_4$ , by using simple  $\text{CO}_2/\text{H}_2$  pulse discharges with Ni catalysis. Further, we examine the possibility of the production of C2 hydrocarbons, such as ethane and ethylene. The production of these materials is demonstrated.

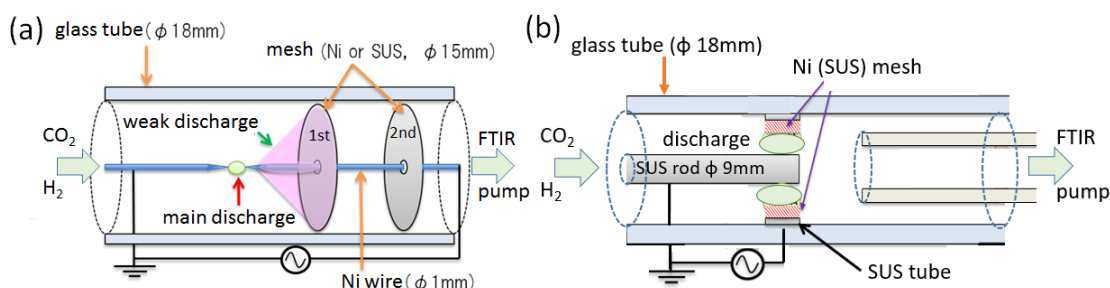
## II. EXPERIMENTAL APPARATUS

Fig. 1(a) shows  $\text{CO}_2$  decomposition device, consisting of a glass tube of 18 mm in inner diameter and a pair of Ni wire electrodes of 1 mm in diameter with a gap of 1 mm. Two mesh discs (1<sup>st</sup> and 2<sup>nd</sup>) of 15 mm in diameter made of Ni or SUS (stainless steel) are placed behind the gap at 4 mm and 14 mm. Mesh size is 100 mesh. Pulse discharge in the axial direction (axial discharge) is performed in Figs. 1(a). On the other hand, a pulse discharge in the radial direction (radial discharge) is performed in an annular space between a SUS rod electrode of 9 mm in diameter at the center, grounded electrically, and a SUS tube powered electrode of 10 mm long, placed just inside the glass tube, as shown in Fig. 1(b). Mixture gas of  $\text{CO}_2$  and  $\text{H}_2$  was supplied to the glass tube by changing discharge parameters under fixed flow rate ratio at  $\text{H}_2/\text{CO}_2 = 5 \text{ sccm}/1 \text{ sccm}$  (standard-state cubic centimeter per minute). The plasma discharge was triggered by applying a negative square pulse voltage to the electrodes. The pulse width is 5  $\mu\text{s}$ . The experiment was carried out by changing the discharge current  $I_d$ , i.e., input discharge power, total gas flow rate, and total pressure. The gas components before and after the discharge were analyzed by FTIR (Fourier transform infrared spectroscopy).

The results were evaluated by the following quantities.

- (1)  $\text{CO}_2$  decomposition ratio  $\alpha$  (%) =  $1 - [\text{CO}_2]_{\text{OUT}}/[\text{CO}_2]_{\text{IN}}$ .
- (2)  $\text{CH}_4$  selectivity  $\beta$  (%) =  $[\text{CH}_4]/[\text{all carbon species produced}]$ .
- (3)  $\text{CH}_4$  production energy efficiency  $\gamma$  (L/kWh) =  $[\text{CH}_4 \text{ in litter}] / \text{electric input energy (kWh)}$  for the discharge.

Electric input power was calculated from a time averaged  $V(t) \times I(t)$  measured directly in the discharge circuit. Here,  $V(t)$  and  $I(t)$  are voltage and current for the discharge at time  $t$ , respectively.



**Fig. 1** Experimental apparatus for (a) axial discharge and (b) radial discharge.

## III. EXPERIMENTAL RESULTS

### 3.1 Effect of discharge types with and without Ni mesh on $\text{CH}_4$ production

First, we examine the effects of discharge types and Ni mesh for  $\text{CH}_4$  production by using the experimental apparatus shown in Figs. 1(a) and (b) for the axial and radial discharges, respectively. Dependence of  $\text{CO}_2$  decomposition ratio  $\alpha$  on discharge current  $I_d$  is shown in Fig. 2(a) for the axial and radial discharges with a use of Ni mesh or SUS mesh. In the case of the axial discharge,  $\alpha$  increases almost linearly with an increase in discharge current  $I_d$  in the range  $I_d \leq 70 \text{ mA}$  as shown by solid lines, where there appears not much difference between Ni and SUS meshes. In the range  $I_d \geq 70 \text{ mA}$ , however,  $\alpha$  in case of Ni mesh becomes higher than that of SUS mesh. On the other hand, in the case of the radial discharge, the increase in  $\alpha$  is rather slow as shown by dotted lines in Fig. 2(a), where also no clear difference is observed between Ni and SUS meshes in the range  $I_d \leq 100 \text{ mA}$ . It is clear that the axial discharge is quite effective for  $\text{CO}_2$  decomposition, about 2 times higher, compared to the radial discharge. Fig. 2(b) shows variation of  $\text{CH}_4$  selectivity  $\beta$  as a function of  $I_d$  for the axial and radial discharges with a use of Ni mesh or SUS mesh. In both discharge cases,  $\beta$  in case of Ni mesh becomes larger than that of SUS mesh. Moreover, it is remarkable that the maximum of  $\beta$  is achieved at a rather low current of 40 mA for the axial discharge with Ni mesh, compared with 85 mA in the case of the radial discharge with Ni mesh. As a result, the energy efficiency  $\gamma$  raises to about 1.1 L/kWh in the case of the axial discharge with Ni mesh as shown in Fig. 2(c). From this experiment it is found that the axial discharge with Ni mesh is quite effective for  $\text{CH}_4$  generation from  $\text{CO}_2$ , compared to the radial discharge.

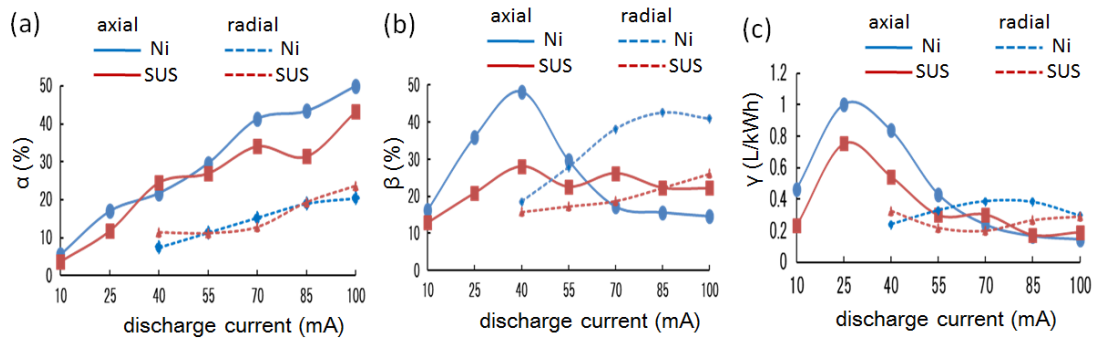


**Fig. 2** Dependences of (a) CO<sub>2</sub> decomposition ratio  $\alpha$ , (b) CH<sub>4</sub> selectivity  $\beta$ , and (c) energy efficiency  $\gamma$  on discharge current  $I_d$  using different mesh materials (Ni or SUS) for the axial and radial discharges.

To examine the effect of total gas flow rate on CH<sub>4</sub> production, variations of  $\alpha$ ,  $\beta$ , and  $\gamma$  are shown in Figs. 3(a), 3(b), and 3(c), respectively, as a function of gas flow rate of CO<sub>2</sub> under a fixed gas flow rate ratio H<sub>2</sub>/CO<sub>2</sub> = 5 for the axial discharge. With an increase in CO<sub>2</sub> flow rate,  $\alpha$  decreases gradually at first, then  $\alpha$  is almost saturated around 13 %, as shown in Fig. 3(a). Variation of  $\beta$  is rather simple, decreasing monotonically from 50 % to about 30 % with an increase in CO<sub>2</sub> flow rate, as shown in Fig. 3(b). However, the energy efficiency always increases with an increase in CO<sub>2</sub> flow rate and reaches the maximum 2.7 L/kWh at 10 sccm. This is reasonable, because  $\gamma$  is proportional to  $\alpha\beta\Gamma$ . Here,  $\Gamma$  is CO<sub>2</sub> flow rate. Therefore, it means that the increase in CO<sub>2</sub> flow rate surpasses the decrease in  $\alpha\beta\Gamma$ . Next, an effect of total pressure on CH<sub>4</sub> production is also examined as shown in Fig. 4 under a fixed gas flow rate ratio H<sub>2</sub>/CO<sub>2</sub> = 5. There appears not much change in values  $\alpha$ ,  $\beta$ , and  $\gamma$  by the change of total pressure. Axial discharge is found to be available even in a sub-atmospheric pressure range of  $2 \times 10^4$  Pa.

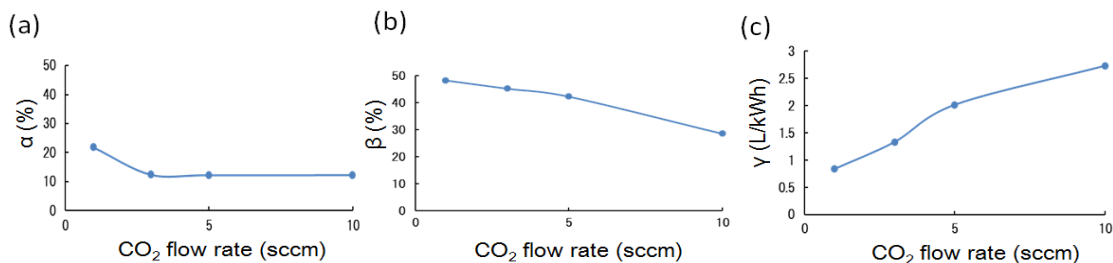


**Fig.3** Dependences of (a) CO<sub>2</sub> decomposition ratio  $\alpha$ , (b) CH<sub>4</sub> selectivity  $\beta$ , and (c) energy efficiency  $\gamma$  on CO<sub>2</sub> flow rate under fixed gas mixture ratio H<sub>2</sub>/CO<sub>2</sub> = 5 for the axial discharge.

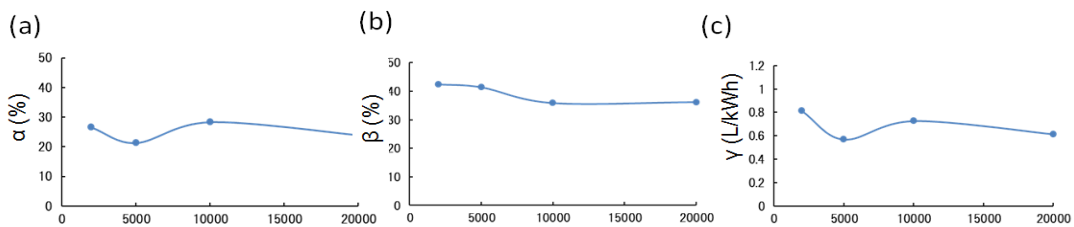


**Fig.4** Dependences of (a) CO<sub>2</sub> decomposition ratio  $\alpha$ , (b) CH<sub>4</sub> selectivity  $\beta$ , and (c) energy efficiency  $\gamma$  on total pressure under fixed gas mixture ratio H<sub>2</sub>/CO<sub>2</sub> = 5 for the axial discharge.

### 3.2 Effect of cathode configuration on CH<sub>4</sub> production

Effect of the powered electrode configuration on CH<sub>4</sub> production is examined by using two kinds powered electrodes. One is the same as shown in Fig. 1(a), consisting of a Ni wire with the 1<sup>st</sup> and 2<sup>nd</sup> Ni mesh disc electrodes. The other is a Ni wire with the 1<sup>st</sup> Ni mesh disc, connected to a Ni mesh cylinder of 10 mm long, placed just on the inner surface of the glass tube, surrounding the gap between Ni wire pair electrodes. In this case, the 2<sup>nd</sup> mesh is removed. The former configuration is a conventional gap discharge with Ni mesh disc behind. On the other hand, the latter configuration is a so-called hollow cathode configuration, where the tip of the powered Ni wire

electrode is surrounded by Ni cylindrical mesh and Ni mesh disc. Figs. 5(a), (b), and (c) show the variations of  $\alpha$ ,  $\beta$ , and  $\gamma$ , respectively, as a function of the discharge current  $I_d$ . It is confirmed that the hollow cathode configuration made of Ni mesh disc and Ni mesh cylinder is quite effective for maximizing  $\gamma$  and reducing the optimized discharge current from 40 mA to 25 mA. In fact, the maximum  $\gamma$  is increased in the hollow cathode configuration at  $I_d = 25$  mA. This is because that owing to the potential varrier provided by a hollow cathode configuration, the electrons in the discharge are well confined in a narrow gap region, which would enhance the dissociation of CO<sub>2</sub> and a resultant increase in the energy efficiency  $\gamma$ .

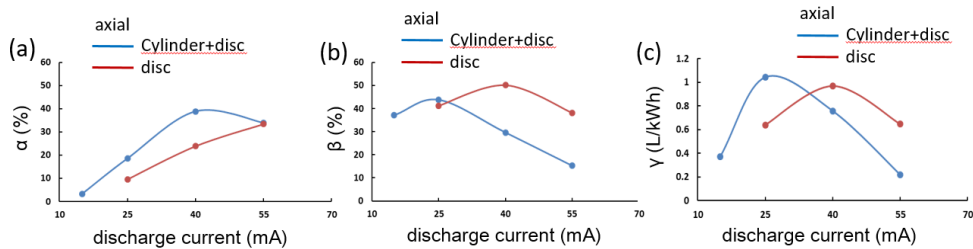


**Fig.5** Dependences of (a) CO<sub>2</sub> decomposition ratio  $\alpha$ , (b) CH<sub>4</sub> selectivity  $\beta$ , and (c) energy efficiency  $\gamma$  on discharge current  $I_d$  for axial discharge with powered electrode consisting of a Ni wire with Ni mesh disc (red) and a Ni wire with Ni mesh disc/Ni mesh cylinder (blue) under gas mixture ratio H<sub>2</sub>/CO<sub>2</sub> = 5.

### 3.3 Production of higher order (C2) hydrocarbons in a closed discharge system

Higher order hydrocarbons such as ethane, ethylene, and acetylene are more valuable because of an inclusion of higher chemical energy in comparison with methane. For this reason, we intend to perform a longer time discharge in a closed gas system for promoting the secondary reactions among methane and hydrocarbons in the discharge. Here, we employ the radial discharge system shown in Fig. 1(b), with a cylindrical Ni or SUS mesh electrode, attached to the inner surface of a tube powered electrode made of SUS. Before turning on the discharge, input and output valves connecting to gas feeding and evacuation pipes, respectively, are closed after packing a mixture gas at the ratio H<sub>2</sub>/CO<sub>2</sub> = 5. Then, after turning on the discharge temporal variation of gas components in the closed system is measured.

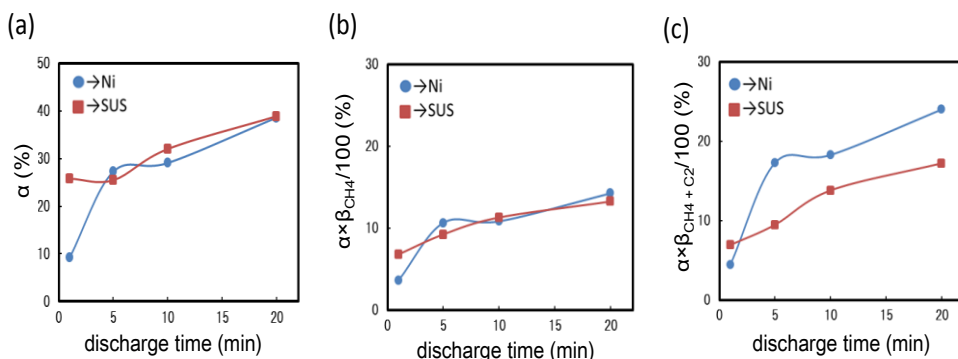


**Fig. 6** Temporal variations of (a) CO<sub>2</sub> decomposition ratio  $\alpha$ , (b) CH<sub>4</sub> selectivity  $\beta$ , and (c) CH<sub>4</sub> and C<sub>2</sub> yield  $\alpha \times \beta_{CH_4+C_2}$  in cases of Ni and SUS mesh electrode for the radial discharge. Initial total pressure is 10 kPa and initial gas mixture ratio is H<sub>2</sub>/CO<sub>2</sub> = 5.

Figure 6(a) shows variations of  $\alpha$  as a function of the discharge time in cases of Ni and SUS mesh electrodes. Although there observed a little ambiguous change in  $\alpha$  just after turning on the discharge,  $\alpha$  gradually increases with time and attains to the maximum  $\alpha \approx 40$  % after 20 minutes. There appears not much difference in  $\alpha$  by the change of the mesh materials. Similarly, as shown in Fig. 6(b),  $\beta$  of CH<sub>4</sub> also gradually increases with time, indicating that the concentration of CO<sub>2</sub> and CO is reducing in time by their reactions with methane produced. As a result, a larger value of total hydrocarbon yield including CH<sub>4</sub> and others C<sub>2</sub>H<sub>m</sub> ( $m = 4, 6$ ) is established in case of Ni mesh, compared with SUS mesh, as shown in Fig. 6(c). It is remarkable that hydrocarbon yield including CH<sub>4</sub> and C<sub>2</sub> attains to the maximum of about 25 % after 20 minutes. Variations of the selectivity of each gas component as a function of discharge time in cases of Ni and SUS mesh electrodes are shown in Fig. 7(a) and 7(b), respectively.

After 1 minute, ethane  $C_2H_6$  is already observed in the discharge with Ni mesh electrode, in spite of the absence of  $C_2H_6$  in case of SUS mesh electrode. Total concentration of  $CH_4$  and  $C_2H_6$  in case of Ni mesh is rather bigger than that in case of SUS mesh. As the discharge further proceeds, ethylene  $C_2H_4$  also appears after 5 minutes in case of Ni mesh, but still almost no  $C_2H_4$  is observed in case of SUS mesh. As can be seen in Fig. 7, the selectivity of CO is reduced in case of Ni mesh, indicating that higher order C2 hydrocarbons are effectively produced on Ni mesh catalysis in the closed discharge by consuming CO and  $CO_2$ .

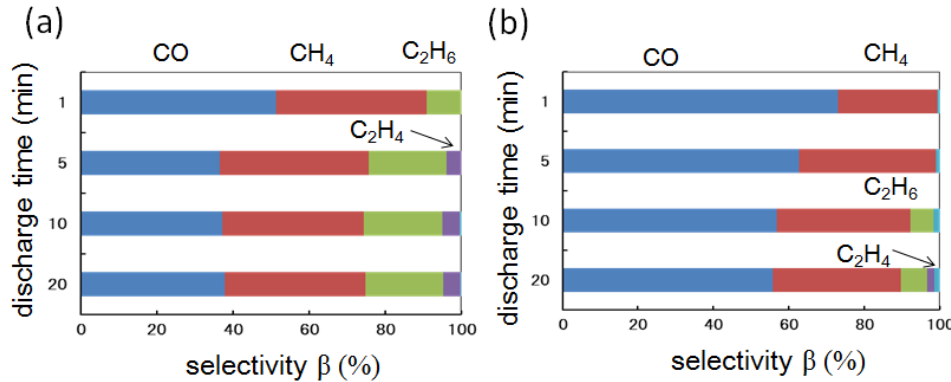


**Fig. 7** Variation of selectivity of each materials as a function of discharge time with (a) Ni mesh and (b) SUS mesh electrodes. Initial total pressure is 10 kPa and initial gas mixture ratio is  $H_2/CO_2 = 5$ .

#### IV. DISCUSSION

The results shown in Fig. 2 are redrawn in Fig. 8 as a function of input discharge power. Variation of  $\alpha$  in a lower power range less than 10 W in case of Ni mesh is not much different from that in case of SUS mesh, as shown in Fig. 8(a). This means that the dissociation of  $CO_2$  is mainly proceeded in the discharge space, i.e.,  $CO_2 \rightarrow CO^* + O^*$  (in discharge), and the dissociation of  $CO_2$  on Ni surface can be neglected. Here, \* denotes radical species in the excited state. Further, regardless of the electrode materials, high values  $\alpha$  were obtained in the axial discharge, compared with radial discharge. This is considered that decomposition of  $CO_2$  is enhanced by an increase in main discharge current density due to a concentration of electric field between pair electrodes. Generally,  $\alpha$  becomes higher in the axial discharge. On the other hand,  $\beta$  in case of Ni mesh in the axial discharge is fairly increased with an increase in input power, compared with that in case of SUS mesh, as shown in Fig. 8(b). This indicates that generation of  $CH_4$  was promoted on Ni surface, in addition to a production in the discharge. In this case, the following reactions are supposed on Ni surface, i.e.,  $CO^*$  (arriving and adsorbed on Ni)  $\rightarrow C^*$  (on Ni) and  $O^*$  (on Ni), then  $C^*$  (on Ni) +  $H_2^*$   $\rightarrow CH_2^*$  (on Ni) +  $H_2^*$   $\rightarrow CH_4$ .

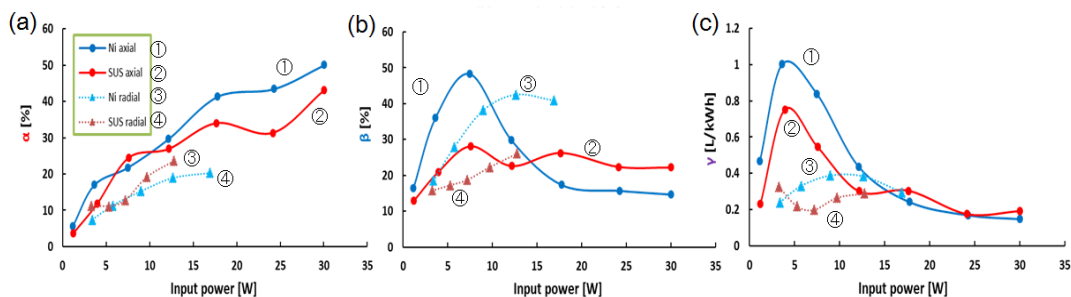


**Fig. 8** Dependences of (a)  $CO_2$  decomposition ratio  $\alpha$ , (b)  $CH_4$  selectivity  $\beta$ , and (c) energy efficiency  $\gamma$  on input discharge power using different mesh materials (Ni or SUS) for the axial or radial discharge. Axial discharges with 1: Ni, and 2: SUS mesh, and radial discharge with 3: Ni and 4: SUS mesh.

In a high power range more than 10 W,  $\alpha$  in case of Ni became larger than SUS. This means that some part of  $CO_2$  is dissociated on Ni surface, resulting in an increase in  $\alpha$  in case of Ni mesh. Conversely,  $\beta$  in case of Ni became lower than SUS. These results were consistently explained by a reversal reaction,  $CO_2 + C^*$  (on Ni)  $\rightarrow 2CO$ , instead of the forward reaction,  $C^*$  (on Ni) +  $H_2^*$   $\rightarrow CH_2^*$  (on Ni) +  $H_2^*$   $\rightarrow CH_4$ . The reversal reaction is triggered by an increase in the surface temperature of Ni mesh. Therefore, methane selectivity  $\beta$  drops much, but

conversely  $\text{CO}_2$  decomposition  $\alpha$  increases in such higher power range. Paying attention to the change of  $\beta$  in case of Ni mesh, the maximum value of  $\beta$  was shifted to a low power side ( $12.7\text{W} \rightarrow 7.5\text{W}$ ) in the axial discharge. As a result, as shown in Fig. 8(c),  $\gamma$  in the axial discharge was raised up to the maximum  $1.1 \text{ L/kWh}$  around  $5\text{W}$ , about 3 times higher than that in the radial discharge.

When the hollow cathode configuration consisting of mesh cylinder and mesh disc is employed, the plasma density effectively increases, resulting in a raise of Ni electrode temperature even in a lower discharge current (power) range. Reasonably higher surface temperature is necessary for catalysis effect. Owing to such increase in temperature, the discharge current for  $\gamma$  becoming the maximum might be shifted to a low discharge current regime, accompanied by an increase in  $\alpha$ , as shown in Fig. 5. Variations of  $\text{CH}_4$  yield  $(\alpha \times \beta)/100$  and energy efficiency  $\gamma$  are shown in Fig. 9. The axial discharge with Ni mesh (red line) is found to give a most efficient operation for the methane production, compared with the radial discharge (blue line). Further, the use of Ni mesh is superior to SUS mesh, in both types of discharge, as described above. We achieved  $\text{CH}_4$  yield  $(\alpha \times \beta)/100 = 10.5 [\%]$  and energy efficiency  $\gamma = 0.84 [\text{L/kWh}]$  simultaneously.

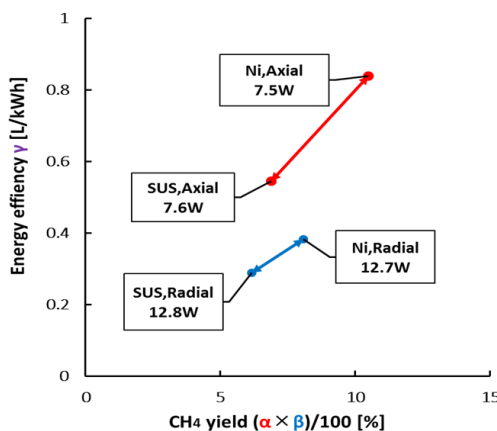


**Fig. 9** Relationship between  $\text{CH}_4$  yield and energy efficacy for  $\text{CH}_4$  production for four cases, i.e., red line: axial discharge with Ni and SUS mesh; blue line: radial discharge with Ni and SUS mesh.

The production of the higher order hydrocarbons such as ethane and ethylene is promoted in case of Ni mesh electrode in the closed discharge system, because the reactants in the gas phase can remain for a long time, compared with the gas flowing system. With an increase in the concentration of  $\text{CH}_4$  in the discharge,  $\text{CH}_4$  is able to react with hydrocarbon radicals on Ni surface, i.e.,  $\text{CH}_4 + \text{CH}_2^*$  (on Ni)  $\rightarrow \text{C}_2\text{H}_6$  and  $\text{CH}_4 + \text{CH}_2^*$  (on Ni)  $\rightarrow \text{C}_2\text{H}_2 + \text{H}_2$ . As a result, concentration of CO in the discharge diminishes, accompanying simultaneous reactions  $\text{CO}^*$  (on Ni)  $\rightarrow \text{C}^*$  (on Ni) +  $\text{O}^*$  (on Ni), and  $\text{C}^*$  (on Ni) +  $\text{H}_2 \rightarrow \text{CH}_2^*$  (on Ni). Methane production occurs basically in the space of discharge, where  $\text{CO}_2$  is decomposed to  $\text{CO}^* + \text{O}^*$  by plasma electrons. Then,  $\text{CO}^*$  is reduced by  $\text{H}^*$  and  $\text{H}_2^*$  radicals for the generation of  $\text{CH}_4$  in the plasma space. However, when Ni catalysis is introduced in the discharge, some amount of  $\text{CO}_2$  and CO, arriving at Ni surface, can be decomposed on Ni surface by the reactions  $\text{CO}_2 \rightarrow \text{CO}^*$  (on Ni) +  $\text{O}^*$  (on Ni) and  $\text{CO}^*$  (on Ni)  $\rightarrow \text{C}^*$  (on Ni) +  $\text{O}^*$  (on Ni). Then, finally both of them are reduced by  $\text{H}_2^*$  and desorbed through the reaction  $\text{C}^*$  (on Ni) +  $\text{H}_2^* \rightarrow \text{CH}_2^*$  (on Ni) +  $\text{H}_2^* \rightarrow \text{CH}_4$ . Therefore, components of  $\text{CO}_2$  and CO in the space of discharge are decreased. Conversely,  $\text{CH}_4$  yield is increased. As a result, both of  $\text{CO}_2$  decomposition ratio  $\alpha$  and methane yield  $\beta$  are increased in case of Ni electrode. Note that Ni has low oxidation potential, compared to SUS (alloy of Fe and Cr). Therefore, desorption of decomposed  $\text{C}^*$  from Ni surface by  $\text{H}_2^*$  reduction would be easier than those from SUS surface. In this way, energy efficiency  $\gamma$  for  $\text{CH}_4$  production in case of Ni electrodes is increased, without using additional heating system for the Ni catalysis. Synergy effect of plasma and catalyst has been established.

## V. CONCLUSION

Effect of discharge type is examined for  $\text{CH}_4$  production. Axial discharge is quite effective compared with radial discharge. This is because in the axial discharge the discharge current is confined within a narrow channel in a space between the electrode gap. Therefore, decomposition of  $\text{CO}_2$  is enhanced by plasma electrons. Further, CO produced has a possibility to react with  $\text{H}_2$  in a residual space of the discharge and even on the Ni surface. Ni acts

as a catalysis for CH<sub>4</sub> formation from CO<sub>2</sub>. The catalysis effect of Ni also well acts for a generation of higher order C2 hydrocarbons in a closed gas discharge system. Ethane and ethylene are generated in the discharge with Ni mesh electrode. The concentration of hydrocarbons in the gas is increased with discharge time. Catalysis effect of Ni is found to be effective for the increases of CO<sub>2</sub> decomposition ratio  $\alpha$ , methane selectivity  $\beta$ , and energy efficiency  $\gamma$  for methane production and even for C2 hydrocarbons production.

## REFERENCES

- [1] The end of fossil fuel, Ecotricity, <https://www.ecotricity.co.uk/our-green-energy/energy-independence/the-end-of-fossil-fuels>.
- [2] Carbon calculator, <https://www.carboncalculator.co.uk/effects.php>.
- [3] L K R Struckmann, A Pesched, R H Rauschenbach, K Sundmacher, Assessment of methanol synthesis utilizing exhaust CO<sub>2</sub> for chemical storage of electrical energy, *Ind. Eng. Chem. Res.* 49, 11073-11078 (2010).
- [4] S. K. Hoekman, A. Broch, C. Robbins, R. Purcell, CO<sub>2</sub> recycling by reaction with renewably-generated hydrogen, *Int. J. Greenhouse Gas Contr.* 4, 44-50 (2010).
- [5] B. Eliasson, U. Kogelschatz, B. Xue, L M Zhou, Hydrogenation of carbon dioxide to methanol with a discharge-activated catalyst, *Ind. Eng. Chem. Res.* 37, 3350-3357 (1998).
- [6] J. H. Lunsford, Catalytic conversion of methane to more useful chemicals and fuels: a challenge for the 21st century, *Catal. Today*, 63, 165-174 (2000).
- [7] W. McDonough, M. Braungart, P. Anastas, J. Zimmerman, Peer reviewed: Applying the principles of green engineering to cradle-to-cradle design, *Environ. Sci. Technol.* 37, 434A-441A (2003).
- [8] V. Gouyard, J Ttibouet, C B Duperyrat, Influence of the plasma power supply nature on the plasma–catalyst synergism for the carbon dioxide reforming of methane, *IEEE Trans. Plasma Sci.* 37, 2342-2346 (2009).
- [9] D W Larkin, L LLobban, R G Mallinson, Production of organic oxygenates in the partial oxidation of methane in a silent electric discharge reactor, *Ind. Eng. Chem. Res.* 40, 1594-1601 (2001).
- [10] D. Mei, X. Zhu, YK. He, J D. Yan, X. Tu, Plasma-assisted conversion of CO<sub>2</sub> in adielectric barrier discharge reactor:understanding the effect of packingmaterials, *Plasma Sources Sci. Technol.* 24, 015011 (2015).
- [11] WFL M. Hoeben, W. Boekhoven, F J C M Beckers, E J M Van Heesch, A J M Pemen, Partial oxidation of methane by pulsed corona discharges, *J. Phys. D: Appl. Phys.* 47, 355202 (2014).
- [12] B Zhu, X S Li, J L Liu, X. Zhu, A M Zhu, Kinetics study on carbon dioxide reforming of methane in kilohertz spark-discharge plasma, *Chem. Eng. J.* 264, 445-452 (2015)
- [13] J. R. H. Ross, Natural gas reforming and CO<sub>2</sub> mitigation, *Catal. Today*, 100, 151-158 (2005).
- [14] M. Mikkelsen, M. Jorgensen, F. C. Krebs, The teraton challenge. A review of fixation and transformation of carbon dioxide, *Energy Environ. Sci.* 3, 43-81 (2010).
- [15] R. Snoeckx, R. Aerts, X. Tu, A. Bogaerts, Plasma-based dry reforming: A computational study ranging from the nanoseconds to seconds time scale, *J. Phys. Chem. C* 117, 4957-4970 (2013)
- [16] R. Dorai, H. Hassouni, M. J. Kushner, Interaction between soot particles and NO<sub>x</sub> during dielectric barrier discharge plasma remediation of simulated diesel exhaust, *J. Appl. Phys.* 88, 6060-6071 (2000).
- [17] X. Tao, M. Bai, X. Li, H. Long, S. Shaung, Y. Yin, X. Dai, CH<sub>4</sub>-CO<sub>2</sub> reforming by plasma – challenges and opportunities, *Prog. Energy Combust. Sci.* 37, 113-124 (2011).
- [18] C. Xu, X. Tu, Plasma-assisted methane conversion in an atmospheric pressure dielectric barrier discharge reactor, *J. Energy Chem.* 22, 420-425 (2013).
- [19] R. Arts, W. Somers, A. Bogaerts, Carbon dioxide splitting in a dielectric barrier discharge plasma: A combined experimental and computational study, *ChemSusChem.* 8, 702-716 (2015).
- [20] S. Fujita, H. Teruma, M. Nakamura, N. Takezawa, Mechanisms of methanation of carbon monoxide and carbon dioxide over nickel, *Ind. Eng. Chem. Res.* 30, 1146-1151 (1991).
- [21] D. E. Peebles, D. W. Goodman, J. M. White, Methanation of carbon dioxide on Ni(100) and the effects of surface modifiers, *J. Phys. Chem.* 87, 4378-4387, 1983.
- [22] M. Araki, V. Ponec, Methanation of carbon dioxide on nickel and nickel-copper alloys, *J. Catalysis* 44, 439-448, 1976.
- [23] D. W. Goodman, R. D. Kelley, T. E. Madey, J. T. Yates JR, Kinetics of the hydrogenation of CO over a single crystal nickel catalyst, *J. Catalysys* 63, 226-234, 1980.
- [24] M. Kano, G. Satoh, S. Iizuka, Reforming of carbon dioxide to methane and methanol by electric impulse low-pressure discharge with hydrogen, *Plasma Chem. Plasma Process.* 32, 177-185 (2012).
- [25] T. Tsuchiya, S Iizuka, Conversion of methane to methanol by a low-pressure steam plasma, *J. Envir. Eng. Technol.*, 2, 35-39 (2013).
- [26] K. Arita, S. Iizuka, Production of CH<sub>4</sub> in a low-pressure CO<sub>2</sub>/H<sub>2</sub> discharge with magnetic field, *J. Mater. Sci. Chem. Eng.*, 3, 69-77 (2015).
- [27] K. Arita, S.Iizuka, Conversion of CO<sub>2</sub> to CH<sub>4</sub> by a pulsed hydrogen plasma shower method, *British J. Appl. Sci. Technol.*, 15(6), BJAST.26169, 1-8, 2016.
- [28] K. Sato, F. Sato, S. Iizuka, Enhancement of CH<sub>4</sub> yield by a sub-atmospheric pulse H<sub>2</sub>/CO<sub>2</sub> plasma with Ni electrodes, *American J. Eng. Res. (AJER)*, 5, No.12, 119-123, 2016.